prepared for the
National Institutes of Health
National Institute of Neurological Disorders and Stroke
Neural Prosthesis Program
Bethesda, Maryland 20892

ELECTRODES FOR FUNCTIONAL ELECTRICAL STIMULATION

Contract #NO1-NS-6-2346

Progress Report #10
April 1, 1999 - June 30, 1999

Principal Investigator
J. Thomas Mortimer, Ph.D.

Applied Neural Control Laboratory
Department of Biomedical Engineering
Case Western Reserve University
Cleveland, OH USA

TABLE OF CONTENTS

SECTION B. DESIGN AND FABRICATION OF ELECTRODES, LEADS AND CONNECTORS 3

B.2.1.2: Polymer-Metal Foil-Polymer (PMP) Cuff Electrodes 3

B.2.4.1: Silicone Rubber Sheeting 5

B.2.5.1: Flexion Testing 5

B.2.5.2: Corrosion Testing 7

B.2.7: "Accelerated" Aging 9

SECTION C. IN VIVO EVALUATION OF ELECTRODES 14

C.1.2.3: Continuous Torque Space 14

References 21

SECTION B. DESIGN AND FABRICATION OF ELECTRODES, LEADS AND CONNECTORS

B.2.1.2 Polymer-Metal Foil-Polymer (PMP) Cuff Electrodes

In order to characterize the laser machined structure in the polymer-metal foil-polymer electrode, simple versions of the platinum serpentine structure were created and tensile tested. These structures were basic serpentine paths with a height of 1 mm, a thickness of 0.1 mm and a spacing of 0.2 mm. These are the same dimensions as the basic loop pattern in the current PMP electrode design. One, two and five path structures were manufactured to determine if the addition of paths had an additive effect on the spring constant. Since the stiffness of the platinum is an important variable to minimize in the cuff fabrication process, this test provided insight into the stiffness added by the basic serpentine conductor design. One of each of the one, two, and five path structures were tensile tested. Another set of one, two, and five path structures were laminated and then tensile tested. A set of the 50µm thick MED-4550 silicone rubber sheeting, which was used in the lamination of the structures, were also tensile tested. The geometry of the samples is shown in Table B.1 and the tensile curves of each sample are compared in the graph in Figure B.1.

Table B.1: The geometry of the platinum and laminated serpentine structures tested are shown in this table. In order for the 7 different samples to be compared, their geometry's were factored out by transforming their tensile curves into stress versus strain. This curve yields the Young's Modulus of each sample (slope of the stress versus strain curve). The moduli are shown below for comparison.

Platinum Structure	Spring Constant	Width	Thickness	Gage Length	Young's Modulus	E Deviation
Tensile Tested	k**	w	t	l	E**	in Regression
	N/mm	mm	mm	mm	N/mm^2	Line
1 path	0.0745	1	0.05	10	14.900	0.003
2 path	0.2625	2	0.05	10	26.280	0.002
5 path	0.7046	5	0.05	10	28.184	0.000
1 path laminated	0.1112	1	0.15*	10	22.240	0.006
2 path laminated	0.489	2	0.15*	10	48.900	0.004
5 path laminated	1.0414	5	0.15*	10	41.656	0.001
MED-4550 silicone	0.0408	6	0.05	25.4	3.454	0.060

*The thicknesses of the laminated structures were considered to be 0.05mm for Moduli comparison

**The slopes of the tensile curves pertain only to the data contained within the range of movement of the cuff components (<18.34 microns)

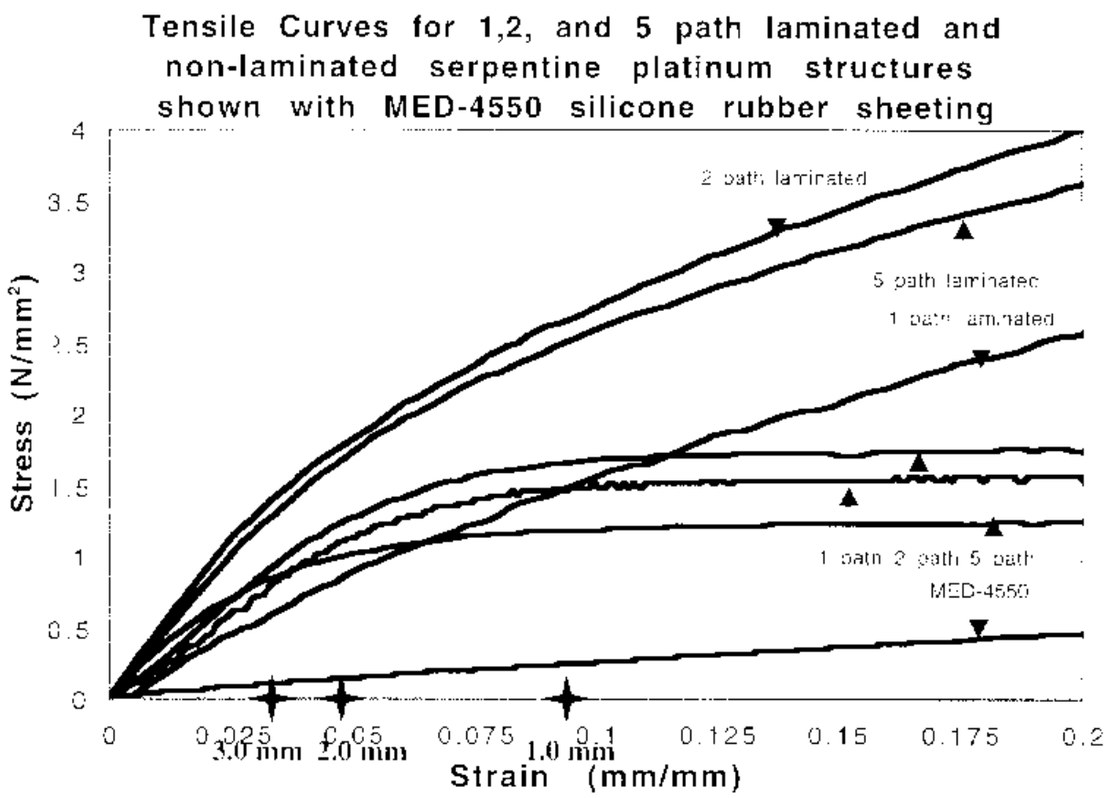

Figure B.1: This graph represents the predicted range of tensile movement for the components within a manufactured 1.0mm inner diameter polymer metal foil-polymer self sizing spiral cuff electrode. The data extends beyond the region shown. The maximum estimated strain that the platinum structure may undergo during manufacture is shown on the graph by the stars for a 3.0, 2.0, and 1.0mm cuff electrode.

The region shown in the graph above represents the expected strain materials would have to accommodate when the cuff curls. The expected strain was calculated by assuming that curling was accommodated by stretching the outside of the cuff. Calculations were performed placing the neutral axis on the extreme edges of the cuff thickness. The maximum movement is seen when the neutral axis is on the inside edge of the stretched layer of the cuff. This calculation is shown below.

The maximum strain the platinum will undergo will occur when the neutral axis is located on the inside of the stretched layer. The platinum structure would be located at a thickness of approximately 0.075 mm from the inside edge. Assuming no change in thickness, the strain can be found by calculating the change in the circumference as follows:

$$\pi[(d-.075)+2(.005)]-circumference$$

$$strain=\frac{\pi[(d+.075)+2(.005)]-\pi(d-.075)}{\pi(d+.075)}=\frac{2(.005)}{d+.075}=\frac{.01}{d+.075}$$

So, when d=3.0mm ⇒ strain=0.0325 mm/mm
d=2.0mm → strain=0.0482 mm/mm
d=1.0mm → strain=0.0930 mm/mm

As seen in Figure B.1, the maximum estimated strains are within the elastic region for the larger cuffs, but in the plastic region for the smaller cuffs. When the strain lies within the plastic range, this indicates that in order for the cuff to curl, the platinum must be plastically deformed and will no return to its original shape by itself. Knowing the maximum strains the platinum has to move to accommodate each cuff size, the structure can be designed in such a way that the elastic region of the curve is extended beyond the strains required. As each new design is made, one structure can be tensile tested to see where the elastic/plastic transition occurs.

The slopes of the elastic regions of the tensile curves were analyzed to test the hypothesis that the mechanical properties are additive as the number of paths are increased. The average Young's Modulus (E) for the three laminated structures was 37.598, and for the non-laminated structures it was 23.122. The average E for two sheets of silicone rubber plus one layer of elastomer (approximated as three sheets of silicone) was 10.542. Adding 10.542 and 23.122 yields 33.664. It then appears that the Young's Modulus of the laminated structure is approximately the modulus of the non-laminated structure plus the modulus of two sheets of silicone rubber sheeting plus a layer of elastomer. The sample size for these structures was only one sample per type of structure. Should a larger sample size be tested, it is hypothesized that the Young's Moduli will grow closer to the additive theory described above.

B.2.4.1 Silicone Rubber Sheeting

The goal of this project was to establish performance specifications for the silicone rubber sheeting used in the spiral cuff electrode fabrication. Tests were conducted to determine the mechanical and physical properties of four different silicone rubber sheeting formulations. Additionally, we investigated the effects of aging and sterilization on these properties.

Results from testing were reported in periods 6 through 9. The relationship between the strain put on the stretched silicone sheet during manufacture and the final inner diameter of the cuff was to be studied further in this period. Due to vendor material problems, we will not be able to complete this study within the timeframe of the contract.

B.2.5.1 Flexion Testing

Simulated Aging with Flexion Test

Four sets of 8 cuffs were placed in four 250 mL flasks containing a phosphate buffered saline solution held at 85°C for 28 days. Each cuff is 4 mm in width and at least 10 mm in length. A gas mixture of 2% O_2, 5% CO_2, and 93% N was continuously bubbled through the flasks. The flasks were set on a hot plate/stirrer. A 3.6 cm magnetic stirrer bar with a 1 cm diameter was placed in each flask and stirred so that the solution formed a vortex approximately

60 mL deep. After a 28-day period, the cuffs were removed and tensile tested to failure. The gage length of the cuffs was 8 mm. Control cuffs, which were not aged, were also tensile tested.

The four sets of aged cuffs were cut from the surrounding silicone material from four different electrode fabrications. These electrodes were part of a batch of ten electrodes that were all fabricated in the same way, using the same materials, and within a two-day period. The control cuff set was comprised of two cuffs from each of the four sets to be aged, and from surrounding material of other electrodes manufactured in the batch of ten described above. The four aged groups and two control groups were later statistically analyzed by combining the aged groups into one and the control groups into one. This was done since it was believed that the only variance between the respective groups would be due to variance in fabrication.

Each set of cuffs, aged and control, were tensile tested. The tensile curves for the cuffs in each set were averaged to obtain average data points which form a tensile curve for each set (2 control sets and 4 aged sets). The first linear region of the curves was studied to determine the spring constant. This region of the tensile curves is shown in the graph below.

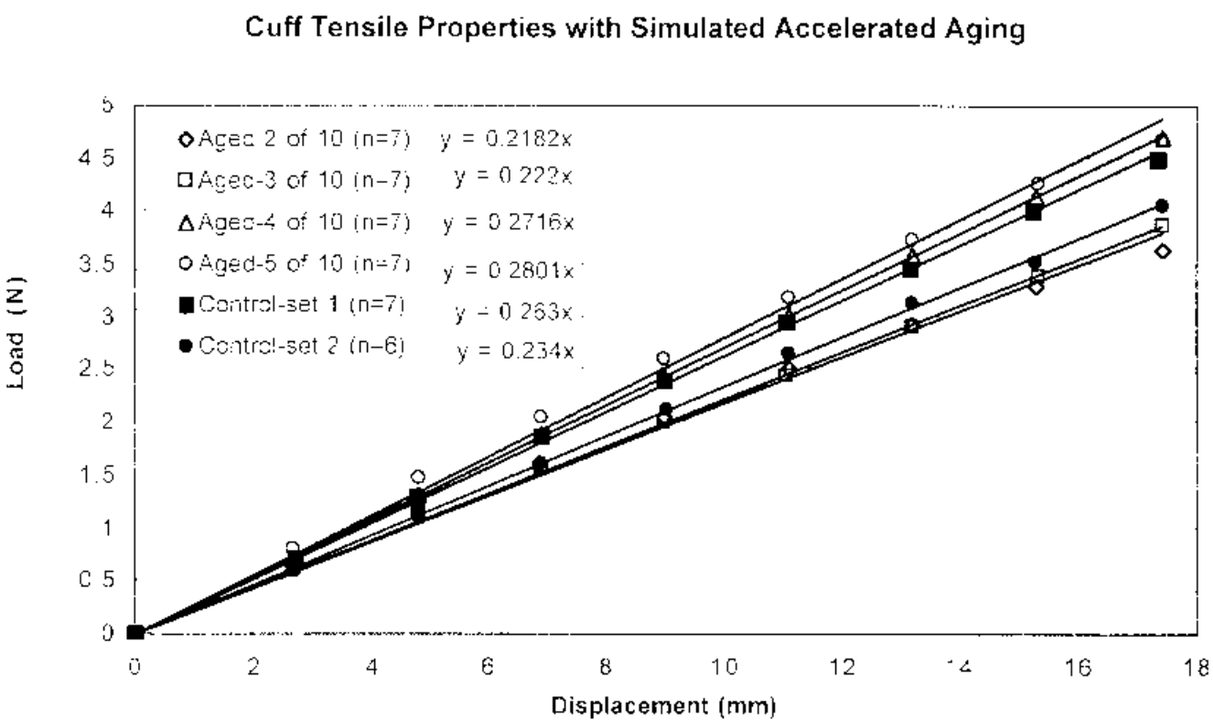

Figure B.2: The graph above contains the first linear region of the tensile curves for the six groups of cuffs studied. The first four on the chart were aged and are named according to the electrode from which the cuffs were taken. It can be seen that the control groups are interspersed with the aged groups.

The spring constants were then found for the two groups of cuffs, aged and control. The spring constants (k) were found by taking the k's for each tensile curve and averaging them. The spring constant for the aged group of cuffs was found to be 0.2514 N/mm^2 and the spring constant for the control set is 0.2458 N/mm^2. A student's t-test assuming equal variances and a null hypothesis that the means are equal was performed on these two data arrays and revealed an alpha of 0.6237 for a two-tailed probability distribution, which means that we cannot claim that the two spring constants are statistically different. Another student's t-test was then performed on the data after adding one standard deviation to the control set. This test produced an alpha of 0.0146. This can be interpreted to mean that the two spring constants are within one standard deviation of one another. We conclude that there was no significant measurable change in the tensile properties of the silicone rubber cuffs after 28 days of simulated accelerated aging and mechanical movement.

Four PMP3 electrodes were also aged in flasks at 85 C for 28 days on a hot plate/stirrer. These electrodes were inspected using visual microscopy. No delamination or damage was observed. The electrodes are also being used in the corrosion testing project (Section B.2.5.2). Once the stimulation is finished, the electrodes will be examined using light microscopy and Scanning Electron Microscopy (SEM).

In addition to testing the cuffs, samples of 75 µm thick silicone sheeting will undergo simulated aging under stress. Sample groups of the sheeting will be control (no aging) and aged with stress. The aged with stress group will contain pieces of silicone rubber sheeting that have been stretched and placed in a frame during aging. Dots of adhesive will be placed on the sheeting before stretching in order to illustrate the change in length after the stretch and after aging. The samples will be placed in a temperature bath at 85 C for 28 days. After the 28-day period, any relaxation in the silicone will be measured by observing the movement of the adhesive markers. This will provide information regarding the self-sizing and inner diameter of the cuff *in vivo*.

B.2.5.2 Corrosion Testing

Samples

Two sets of four electrodes are being tested for corrosion. One set contains electrodes that have undergone simulated aging. These are the four electrodes tested in the Simulated Aging/ Flexion test of Section B.2.5.1. The other set contains two electrodes that were used in the rolling test (Section B.2.5.1). These samples represent electrodes that have been flexed beyond what is expected during manufacture and implant. They will provide information on the relationship between fatigue from flexion and corrosion. The remaining two samples are unused, meaning they have not been flexed, aged, or tested since manufacture.

Stimulation

Four electrodes (sets of two running in parallel) are pulsed at the maximum expected stimulus parameters. Specifically, they are pulsed continuously at 20 Hz with biphasic, charge balanced, capacitive coupled, rectangular waveform at 3 mA with 10µs pulsewidth and 0 interphase delay. One electrode (4 contacts) receives 3 anodic currents and 1 random control (no pulsing). The second electrode receives 3 cathodic currents and 1 random control. The resulting voltage between each electrode contact and a saturated calomel reference electrode is measured

using high input impedance (10^{12} Ω) buffer amplitudes and an RMs voltmeter. These measurements are taken twice each week.

Bath & Medium

The test is run in a bath of phosphate buffered saline solution. A gas mixture of 2% Oxygen, 5% Carbon Dioxide, and 93% Nitrogen is continuously bubbled through the flasks. The set-up for the test is shown in the figure below.

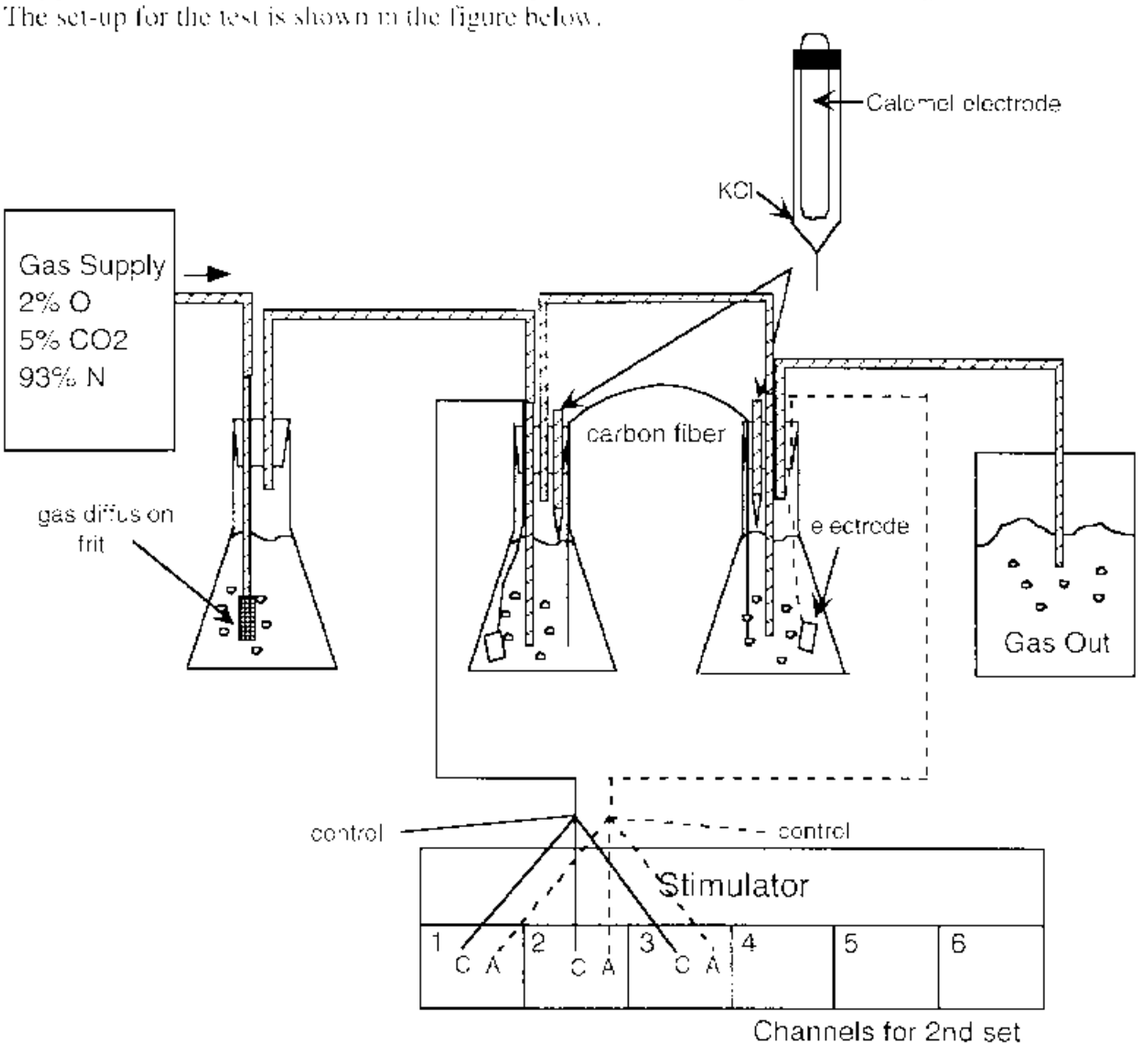

Figure B.3: The schematic above illustrates the gas flow and electrical connections for the electrochemistry corrosion test. The ports shown for the insertion of the calomel electrode are also used to add ultrapure water if necessary and to take samples for analysis. The "C" and "A" on the stimulator stand for Cathodic and Anodic currents. One of the leads, the control, is not connected to the stimulator. Carbon fiber bridges the electrodes allowing for current to pass between flasks. Two more electrodes are run simultaneously using the same setup. The parameters for this test are a current of 3 mA, a pulsewidth of 10 µs, a frequency of 20 Hz, and a charge density of 15 µC/mm^2.

Testing

The amount of platinum in solution will be tested before the test begins and after the 28 day period. SEM will be performed on a control group of three electrodes (12 stimulation sites) that have not been tested. Microscope inspection and SEM will also be performed on the stimulation sites of the tested electrodes (32 sites) and on any suspected corrosion sites (remove insulation). This evaluation will take place after the 28-day test period. Deposits of corrosion will also be examined for elemental composition using EDAX. The electrodes will also be examined for delamination.

Results

The first set of four electrodes completed the 28 day stimulation. These electrodes were removed from the saline solution, allowed to dry, then cleaned and inspected using light microscopy. They were also examinated using scanning electron microscopy. Results from comparison of the condition of the stimulation sites after the stimulation and the control pictures will be discussed in the next report.

The amount of platinum in the phosphate buffered saline solution was also measured before and after the 28-day period. The carbon fiber electrodes were also tested for platinum at the end of the 28-day test. No platinum was detected in the baseline samples. There was also no platinum detected in the 28-day samples. The detection limit for platinum was 0.1 µg per mL of solution. These results were interpreted to indicate that if corrosion occurred during the 28-day period it was below our detection limits.

In order to predict the life of this electrode, it is useful to consider a typical stimulus regime for a prosthetic device. Estimates of hand grasp prosthesis use report that the system requires 200,000 pulses per day, totaling 365 million pulses over a five-year period. The PMP electrodes tested were stimulated at a rate of 20 pulses per second over a 28-day period. This equates to 48,384,000 pulses delivered to each contact stimulated. Three contacts were stimulated per electrode which, when added, equals 145,152,000 pulses. Because there was no loss of platinum, within the detection limit, it is reasonable to say that the electrode should last at least 2 years.

B.2.7 "Accelerated" Aging

Polymer performance is directly related to how its structure, and therefore mechanical properties, change with time. It is desired to find a relationship between the time a polymer is in use, or stored, and the temperature at which it is used or stored at. This relationship would allow for an accurate way to perform accelerated aging tests. In other words, a polymer could be raised to an accelerated temperature over a short period of time in order to simulate the aging it would see over a longer period of time.

We at the Applied Neural Control Laboratory at Case Western Reserve University have been searching for ways to estimate if our electrodes will "hold up" inside the body for a given number of years. We would like to be able to tell any interested party what the life expectancy of our electrode is. Currently, the only accurate way of measuring electrode life is to implant the electrode *in vivo* and determine when it fails. This process could take many years. Improved devices and material changes are occurring rapidly in the field of biomedical engineering. Because of this, it is necessary to accelerate the aging process so that a life expectancy estimate can be made within a more timely period, such as a few months. Such accelerated aging

processes have been performed previously by increasing the temperature that the specimen is held at. In order to make such an estimate, a relationship between time and temperature appropriate for polymers must be found.

Researching temperature accelerated aging revealed three categories of methods that have been used, or are suggested to be used for the "accelerated" aging of polymers. These models are the Larsen-Miller model, Arrhenius based models developed by Hemmerich, NAMSA, and Edel, and a model to develop a relationship unique to an application referred to as the D&A model. Most of these methods have origins or are based on the Arrhenius rate law. This law states that the rate of a simple (first-order) chemical reaction depends on temperature and is stated according to Nelson as follows:

$$\text{Rate} = A' \exp[-E/(kT)].$$

where E = the activation energy of the reaction
k = the Boltzmann's constant (8.617x10^{-5} electron volts per °C)
T = the absolute Kelvin temperature
A' = a constant that is characteristic of the product failure mechanism and test conditions.

A model that has been used previously was a time-temperature relationship developed by Larsen and Miller in 1952. This relationship is based on the effect of temperature on time to creep. It was developed for the life prediction of alloys. It was known that creep, tempering, and diffusion all obey rate-process theories. The Larsen-Miller relationship is given by the following:

$$T_a(20+\log t_a) = T_s(20+\log t_s)$$

where T_a = ambient temperature
t_a = time duration at ambient temperature
T_s = aging temperature
t_s = time duration of aging.

This relationship was shown by Larsen and Miller to work for metals with good accuracy. The theory relates aging to creep, which means that if the molecules in a given material are moving away from one another at high temperatures (creep) then the material is being aged at an accelerated rate. It seemed logical that creep was responsible for the degradation occurring in our polymers. Although we may be aging the material, we are not certain as to the particular relationship between the temperature and the time since the theory described above relates specifically to metals.

In July of 1998, the Medical Plastics and Biomaterials magazine published an article on an aging theory for medical devices. The author, Hemmerich, develops a theory for ensuring the performance of polymers after being stored for a length of time. This model, later referred to as the Hemmerich model, was developed around the collision theory-based Arrhenius model. The model is as follows:

$$TIME_{T1} = \frac{TIME_{RT}(10)}{Q_{10}(T - T_{RT})}$$

where T = aging temperature
T_{RT} = ambient temperature
$TIME_{T1}$ = time duration of aging
$TIME_{RT}$ = time duration at ambient temperature
Q_{10} = reaction-rate coefficient.

A reaction-rate coefficient of 2.0 is the generally accepted rate for a first order chemical reaction. 1.8 is a conservative rate and 3.0 would be an aggressive rate for this model.

At first, this model seemed to be the answer to our question of accelerated aging. It was specifically developed for polymers, and although it looks at shelf life of polymers, this could easily be used for an *in vivo* representation as well. Unfortunately, the author suggests an upper temperature limit for the accelerated testing of 60°C. This limit only allows an acceleration rate of 4.6, which limits the benefit of the accelerated testing. The reason for this limit is explained by Hemmerich, "... the accuracy of the assumptions on which this method is based declines sharply as greater geometric multiplication factors are applied with greater deviation from ambient temperature." This statement leads to the conclusion that the model proposed by Hemmerich is not accurate above 60°C.

We also contacted David Parenti at NAMSA who works with accelerated aging testing for the shelf-life of medical devices. According to Mr. Parenti, the model that NAMSA uses to determine the acceleration rate is as follows:

$$TIME_1 = \frac{TIME_2}{2^{(T1-T2)/10}}$$

where TIME = time duration of aging
$TIME_2$ = time duration at ambient temperature
T1 = aging temperature
T2 = ambient temperature.

This model is also only recommended for a T2 of 60°C or less for the same reasons as stated by Hemmerich above. Both of these models are based on the Arrhenius equation, which concurs with the temperature limit. It is also important to note that the accelerated aging that is dealt with in the Hemmerich article and by NAMSA is all shelf life testing of polymers. However, it is believed that these models can be used for the *in vitro* simulation of an *in vivo* model by using the temperature within the body instead of the room temperature.

David Edel, a fellow NIH contractor in the neural prosthesis program at MIT uses a life-temperature relationship based on the Arrhenius Acceleration Factor. Assuming a first-order chemical reaction degradation process, it states

$K=\exp\{(E/k)[1/T_1-1/T_2]\}$;

where K = Arrhenius acceleration factor between the lives at each temperature
E = the activation energy of the reaction (assumed to be 1eV)
k = the Boltzmann's constant (8.617×10^{-5} electron-volts per °C)
T_1 = ambient temperature
T_2 = aging temperature.

The result of this calculation is that the specimen being tested will run K times longer at T_1 than at T_2. David Edel has used the model at aging temperatures above 60°C.

The last model to be discussed here is referred to as the D&A model. It is named after authors Donohue and Apostolou and develops a model unique to a particular specimen by using past data. Specifically, the model requires at least three sets of data at different temperatures. These data are usually from mechanical properties testing of a specimen after being aged for a period of time at a particular temperature. With three different sets, the data can be plotted and a rate equation can be developed according to the graph of the data. In order for this to work, there must be a change in the mechanical properties of the specimen. It is unknown how long our electrode would have to be aged before significant changes would occur which would allow for such a derivation.

In order to compare the models discussed above, calculations were performed for predicting the life of a specimen if held at a temperature of 85°C for 28 days. This information is contained in the table below.

Table B.2: Comparison of Accelerated Aging Models at 60°C and 85°C for 28 days

Model	Author, Year	Accelerated Aging		Predicted Aging	
		Temp (C)	Time(days)	Time(days)	Time(years)
Creep	Larsen&Miller, 1952	60	28	1101.5	3.02
Arrhenius Based	Hemmerich, 1998	60	28	129.2	0.35
	NAMSA, 1998	60	28	138.5	0.38
	David Edel, 1998	60	28	371.6	1.02
D&A	Donohue&Apostolou, 1990	60	28	N/A	N/A
Creep	Larsen&Miller, 1952	85	28	59055.0	161.80
Arrhenius Based	Hemmerich, 1998	85	28	269.1	0.74
	NAMSA, 1998	85	28	783.3	2.15
	David Edel, 1998	85	28	4236.2	11.61
D&A	Donohue&Apostolou, 1990	85	28	N/A	N/A

We have chosen a test set-up for aging at 85°C for 28 days. According to the Hemmerich model this would only simulate 0.74 years. According to the Larsen Miller model, this simulates 161.8 years. Therefore, we believe that the polymers that are tested using the above parameters, are being aged somewhere between 28 days and 161.8 years.

In accelerated aging, the medium that the material is aged in should be as similar to the actual environment as possible. In the past we have been using a phosphate buffered saline solution as our aging medium. NAMSA also uses a saline solution, but specifically note that saline mimics blood. We are not putting our electrodes in blood,

they are implanted within the extracellular fluid (ECF). So, in order to simulate the electrode's aging within the body, we need to use the medium that is the most similar to extracellular fluid. According to Guyton, the composition of extracellular fluid is as shown in the table below. Three solutions that mimic ECF are also shown.

Table B.3: Comparison of Osmolarity in Extracellular Fluid (ECF), Artificial Cerebral Spinal Fluid (ACSF), Pseudoextracellular Fluid (PECF), and Phosphate Buffered Saline Solution

Ions	ECF	ACSF	PECF	Saline
	(mOsm/liter of H2O)			
Na+	139	150	145	271.8
K+	4	4.25	5	0
Ca++	1.2	2	0	0
Mg+	0.7	2	0	0
Cl-	108	141	118	150.1
HCO3-	28.3	26	30	0
HPO4- H2PO4-	2	1.25	2	65
SO4-	0.5	2	0	0
Dextrose	0	10	0	0
Amino Acids	2	0	0	0
Creatine	0.2	0	0	0
Lactate	1.2	0	0	0
Glucose	5.6	0	0	0
Protein	0.2	0	0	0
Urea	4	0	0	0
Others	3.9	0	0	0
Total mOsm/liter	**300.8**	**338.5**	**300**	**486.9**
pH	**7.3**	**7.4**	**8.2**	7.3

Previous work done with accelerated aging used what is termed a Pseudoextracellular Fluid (PECF). This is a medium that is very similar to ECF for the ion concentrations, but has a higher pH. This raise in pH is caused by the absence of protein buffers. Aging mediums have since improved by including the proper amount of buffers. Artificial Cerebral Spinal Fluid (ACSF) is a solution that can be mixed in any laboratory and is also close to ECF. The ion concentrations in ACSF are very similar to ECF and the pH is almost exactly what is found in the human body. Most researchers use saline or phosphate buffered saline solution. One attempt was made to use ACSF which appeared to be a closer match to ECF than the saline. Using the ACSF at elevated temperatures resulted in the formation of a precipitate. Until a better medium is found, the phosphate buffered saline solution will be used for *in vitro* testing to simulate life within the extracellular fluid of the body.

Overtime, gases diffuse out of the solution. In order to keep the solution close to ECF, gases can be added, or "bubbled through" the solution. The best match of ECF is to bubble through the solution a mix of 2% Oxygen, 5% Carbon Dioxide, and 93% Nitrogen. This mixture is continuously bubbled through the aging medium.

SECTION C. IN VIVO EVALUATION OF ELECTRODES

C.I.2.3: Continuous torque space

Abstract

The objective of this project was to develop methodologies to produce a range of torque output with a nerve cuff electrode. The ability to produce a range of torque outputs is needed, in a neural prostheses, to produce the complex muscle-activation patterns that are required to restore function. Based on the good results achieved with the present muscle based (Intramuscular and Epimysial) electrodes, additional function is desired. These present muscle based systems require one electrode and lead wire for each muscle desired for neural prostheses recruitment. A nerve-based electrode offers the potential of activating many muscles with a single electrode. Previous studies have shown that nerve cuff electrodes have the potential of activating many different muscles served by the nerve, individually and independently. By adding the individual outputs produced by these electrodes, complex activation patterns used by neural prostheses can be produced.

Activation of multiple muscles can be achieved using stimulation from a multiple contact nerve cuff electrode. The set of motor neurons that are activated can be shifted within the nerve by varying the level of stimulation applied to different contacts within a multiple contact cuff electrode. In order to avoid the interaction of multiple field potentials, each stimulation pulse must be offset from each of the other stimulation pulses. This study targeted a delay between pulses that would satisfy two conditions. The first condition was that axons, not activated by either stimulus alone, were not activated by the combination of both pulses. The second condition was that no single axon was activated multiple times when the combined simulation was applied. In all 33 trials performed on the sciatic nerves of 4 cats, a range of values for the delay between pulses existed that satisfied both conditions. Delays between 700 and 900μsec were within the desired range of delays in all 33 cases.

The ability to add the output from two different stimulation pulses was tested in five animals. In each animal, a pair of electrode configurations that were believed to activate two different fascicles were tested individually and together. At least five different amplitude combinations were applied to the two different stimulation configurations in each case. For each amplitude set, individual stimulation of both configurations was performed before and after each combined stimulation. The output of the combined stimulation was then compared to the summation of the outputs produced by each individual stimulation. In 125 out of 129 trials across the five different animals, the combined stimulation was found to be within the 98% confidence interval of the sum of the outputs produced by each individual stimulation. The importance of using configurations that activated different fascicles was demonstrated by testing two configurations that were believed to activate the same fascicle. When one configuration was stimulated at an amplitude believed to produce activation of a neighboring fascicle, 4 out of 6 trials produced a combined stimulation that was outside of the 98% confidence interval for the sum of the outputs produced by each individual stimulation. Based on this study, a delay between stimulation pulses (of 900 μsec for the cat sciatic nerve) can be used to achieve a wide range of torque outputs based on only a few different output configurations.

Progress

The objective of this work was to first determine if a single delay time can be successfully used for all stimulation sets performed on the cat sciatic nerve with a nerve cuff electrode. Secondly, identify a specific delay, if one exists, which can be used for all stimulation sets. The work in this section was performed using each of the four contacts located around the sciatic nerve trunks of four different animals. In each run, the delay between two 10μsec pulses applied to the same contact was varied. Each set was analyzed to determine the beginning and end of the plateau region indicating the end of the facilitative region and the end of the refractory region, respectively. An example of one set of data is illustrated in Figure C.1. In Figure C.1, delays up to 75μs were in the facilitative region. Delays between 75μs and 3000μs were found to produce a plateau. This plateau indicates that the facilitative period is over but the end of the refractory period has not occurred yet. At a delay of 3000μs the torque output was found to increase, indicating the refractory period for some of the activated axons had ended. In every set of data, a plateau was observed, indicating that the refractory region was consistently greater than the facilitative region. A cumulative histogram of all of the delays corresponding with the ends of the facilitative and refractory regions from 33 sets of data are illustrated in Figure C.2. A region between 700 and 900 μsec delay was found to be after the end of the facilitative region for all cases but before the end of the refractory region in all cases.

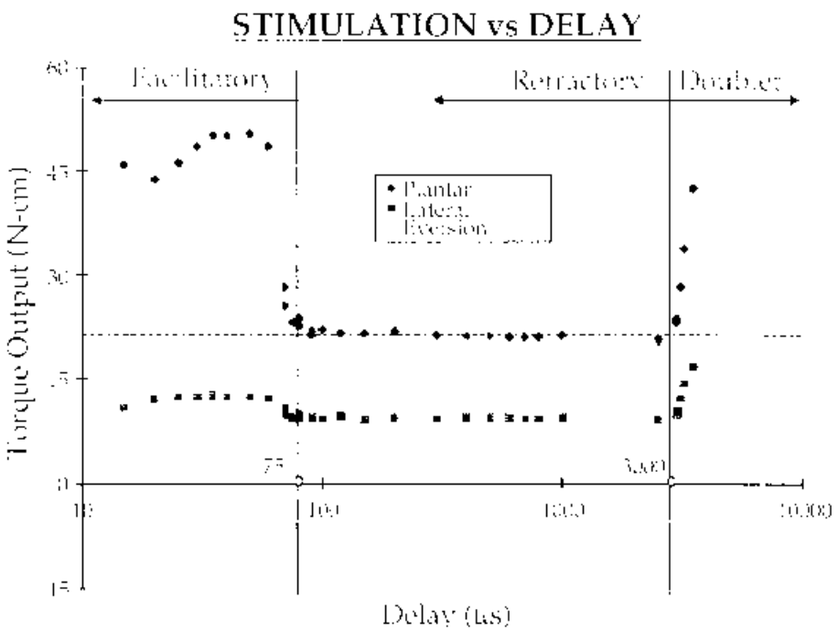

Figure C.1– The torque output produced by two identical stimulation pulses applied through the same electrode configuration is shown based on delay between the two pulses. The facilitatory period, where nerve fibers partially depolarized by the first pulse but then fully activated by the second pulse, was found to last up to 75μs in this case. The refractory period, where nerve fibers that were fully activated by the first pulse could not be activated by the second pulse, was found to last up to 3000μs in this case. The doublet region refers to the time after the end of the refractory period when some nerve fibers had two action potentials produced.

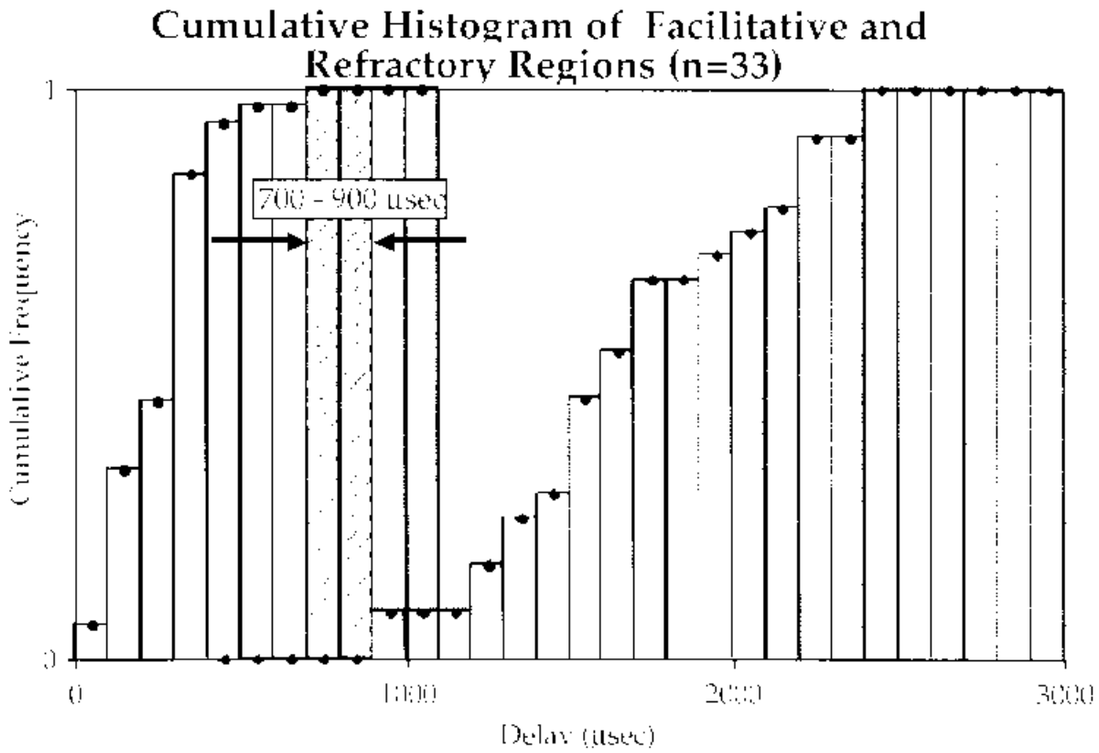

Figure C.2 – This graph is a cumulative histogram of the delays that indicate the end of the facilitative region and the refractory region in 33 data sets acquired across four animals. A region between 700 and 900 μsec delay was found to be after the facilitative region and before the end of the refractory region in all cases.

Using a 900μsec delay between two mutually exclusive stimulation pulses, the resulting net output was compared to the linear summation of the individual torque outputs that were produced by each individual stimulation. The length of the delay was based on the preceding work such that the second pulse would fall after the facilitative period but before the end of the refractory period of the first pulse. Mutual exclusion was based on using stimulation configurations that were believed to stimulate two different fascicles at amplitudes that were below spillover. Each stimulation of the configurations (with a 900μsec delay) using a particular set of amplitudes, was both preceded and followed by stimulation of each configuration alone. An example of combined stimulation using the 900μsec delay between stimuli applied to two different contact configurations is illustrated in Figure C.3. The two thick lines represent the torque output due to one configuration alone. The nerve schematic in the upper left corner is used to illustrate the belief that the Ia configuration stimulated the tibial fascicle (Tib) and the Ib configuration stimulated the medial gastrocnemius fascicle (MG). The actual cross section is not at this time known since the nerve in the animal these data were collected from has not yet, at the time of this writing, been explanted. The lines shown in Figure C.3 represent a torque output produced by an individual configuration and each intersection, of either the solid lines or the dotted lines, is a location where a combined stimulation would be predicted. A total of 7

amplitude combinations (number of locations where similar lines cross) are shown in this figure. In each case the actual and predicted torque output were found to be within the 98% confidence interval of each other. Between 5 and 22 combinations of amplitudes were performed on 10 different pairs of electrode configurations across 5 different animals for a total of 129 data sets. For each combined stimulation, a predicted output was calculated as the sum of the torque outputs resulting from stimulation of the individual configurations. In each case the difference between the actual and predicted torque outputs were compared in each individual dimension (plantar flexion, lateral rotation and eversion). Previous work found the 98% confidence interval for plantar flexion, lateral rotation and eversion to be 5, 2.5 and 1.7 N-cm, respectively. Figure C.4 is a histogram of the differences in the torque produced in each dimension. The dotted vertical lines indicate the location of the 98% confidence interval for each dimension. The number above each region indicates the number of times the difference between the actual and the predicted torque outputs were found to occur in that region. Of the 129 "sums" performed, only 4 cases were found to have even one difference fall outside of the respective confidence region. Of the 4 cases found in Figure C.4, 1 occurrence was found in plantar flexion, 2 occurrences were found in lateral rotation and 1 occurrence was found in eversion.

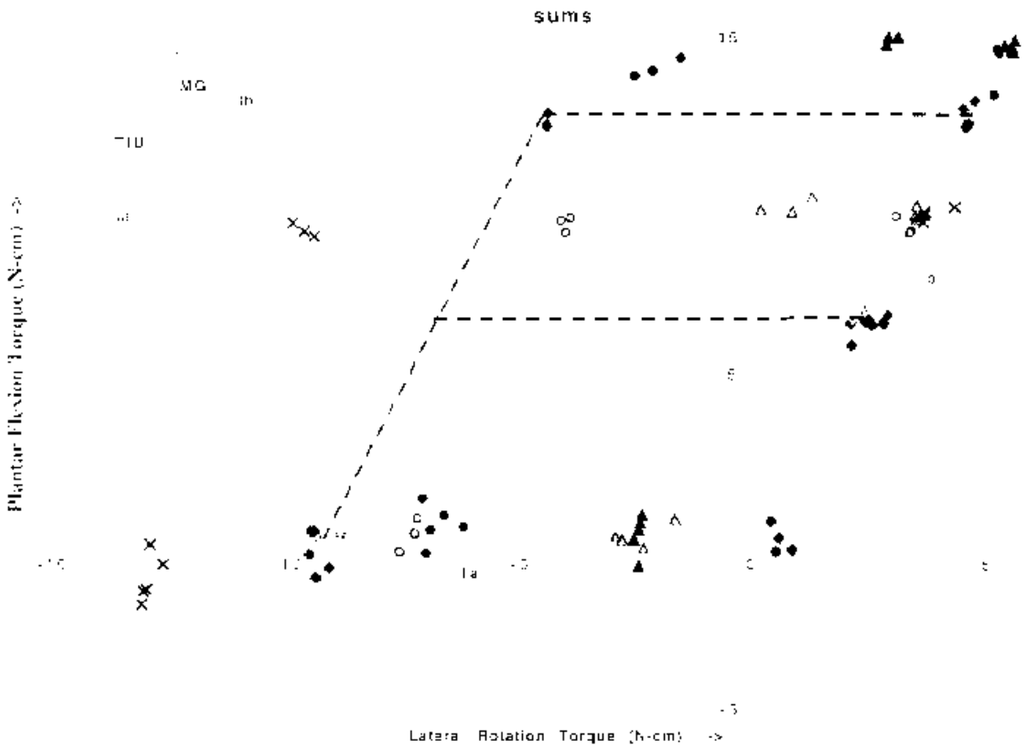

Figure C.3 – This graph is an example of the use of two different configurations with a 900µsec delay to produce a summation of the torque outputs from each of the individual configurations. The two thick lines represent the torque output due to one configuration alone. Each intersection between two solid lines or two dotted lines is a location where a combined stimulation would be predicted and found. A total of 7 amplitude combinations (number of locations where similar lines cross) are shown in this figure.

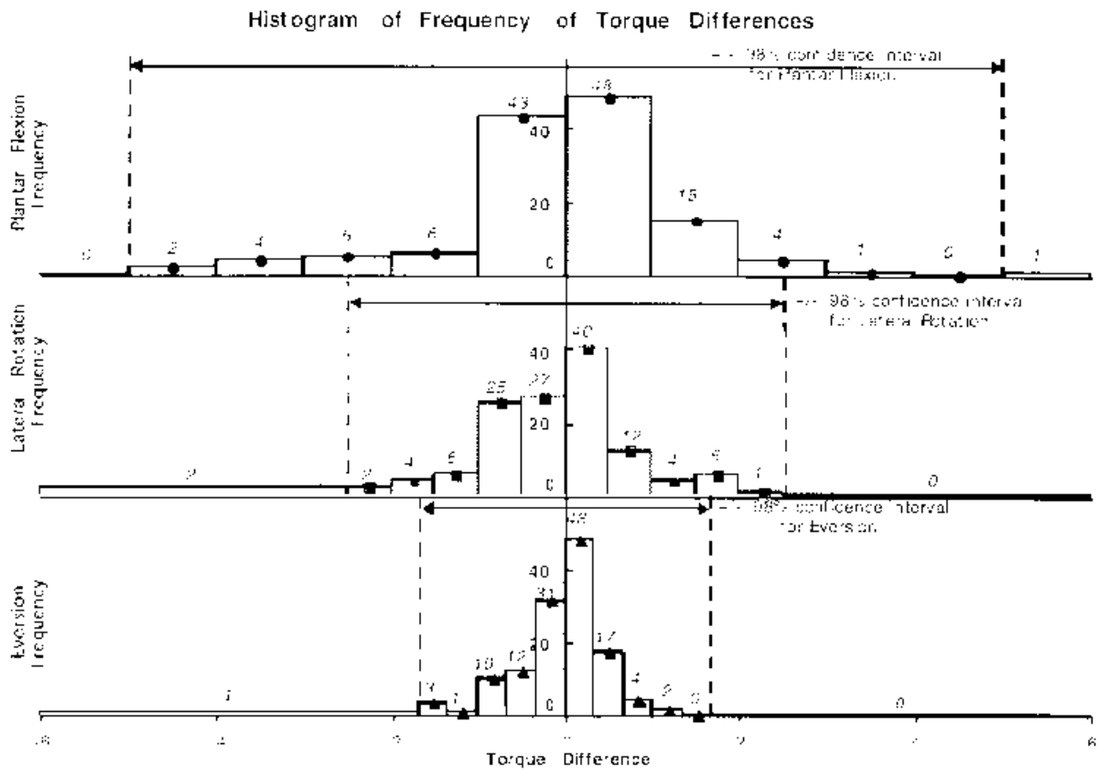

Figure C.4 This is a histogram of the number of times the difference between the actual torque output and the predicted torque output occurred within each region. The predicted torque output was based on the linear summation of each individual torque output. The 98% confidence intervals are shown for the plantar flexion, lateral rotation and eversion dimensions. A total 4 of the 129 differences were found to be outside the 98% confidence intervals.

Discussion

A foreseeable usage for nerve cuff electrodes is for the user (patient, engineer or doctor) to desire a particular torque output to produce a desired motion. By applying stimulation to multiple contacts, each of which activated different sets of nerve fibers, a range of torque outputs were produced.

The use of a time delay was designed to make use of the refractory and facilitative periods after stimulation. The refractory period of an axon is the time after an action potential during which the axon can not produce another action potential. The facilitative period is the time after a stimulation during which an axon, which does not reach the threshold for producing an action potential, remains partially depolarized. During the facilitative period, a stimulation that would normally be insufficient to produce an action potential in the particular axon may produce an action potential due to the axon being partially depolarized. If two pulses are separated by a delay that is greater than the length of the facilitative period but less than the length of the refractory period, the exclusive sum of the two torque outputs should be achieved. In the case that the two individual stimulations activate exclusive sets of axons (i.e. two different fascicles), the net output should be a linear summation of the two individual outputs. This work

was designed to test the hypothesis that by using a delay greater that the facilitative period but within the refractory period, two stimulation pulses can be used to produce an additive output. A delay between 700µs and 900µs was found to be after the facilitative period but before the end of the refractory period for stimulation from a nerve cuff electrode on the cat sciatic nerve. These results fall within the ranges found by Peckham [1972] using intramuscular electrodes in rats and humans and Liang *et al.* [1991]. Ratten *et al.* [1991], and Yoshida and Horch [1993] using intrafascicular electrodes.

Based on the data presented in Figure C.4, the sum of the torque produced by two mutually exclusive stimulation configurations with a 900µsec delay was found to produce a torque output that was essentially the linear summation of the torque produced by each individual stimulation. In 6 cases, stimulation was applied when one of the stimulation configurations were considered above spillover to investigate the result when the two stimulation configurations are not mutually exclusive. The measured torque output from the combined stimulation was found to differ from the predicted torque output by more than the 98% confidence interval in 4 of the 6 cases. In Figure C.5, the 4 cases are broken down into 2 cases where the current applied to configuration Ia was 2.4mA (open arrow) and 2 cases where the current applied to configuration Ia was 2.7mA (solid arrow). The dotted vector lines approximate the expected torque output based on what stimulation of the Ia configuration alone produced. In the two cases in which the difference was not found to exceed the confidence interval (noted by the vertical arrows), the stimulation labeled Ia in Figure C.5 was at a very low level. It is possible that even though one stimulation may have been spilling over to the adjacent fascicle, the actual set of axons stimulated by the two individual stimulation configuration may have still been partially or completely mutually exclusive. This concept is illustrated in the upper left corner of Figure C.5. Configuration Ib may have activated fibers in the tibial (TIB) fascicle that were not activated by the Ia configuration. This is only an illustration of one possibility and is not necessarily the actual orientation of the fascicles within the nerve since this nerve has not yet been explanted.

Based on this work, a linear summation of multiple stimulation outputs can be produced by applying a delay between the two stimulation pulses. In the cat sciatic nerve, a 900µsec delay was found sufficient. If the two stimulation configurations are not mutually exclusive in the axon population that they activate, the net output will not be the simple sum of the two individual outputs. This concept has been used by other investigators as a measure of stimulation overlap [Liang, *et al.* 1991, Ratten, *et al.* 1991, Yoshida and Horch 1993]. Using the technique presented here, a control system can be developed for an end user to produce any range of output within the physiological range. The net result should be an increase in the functionality of new neural prostheses.

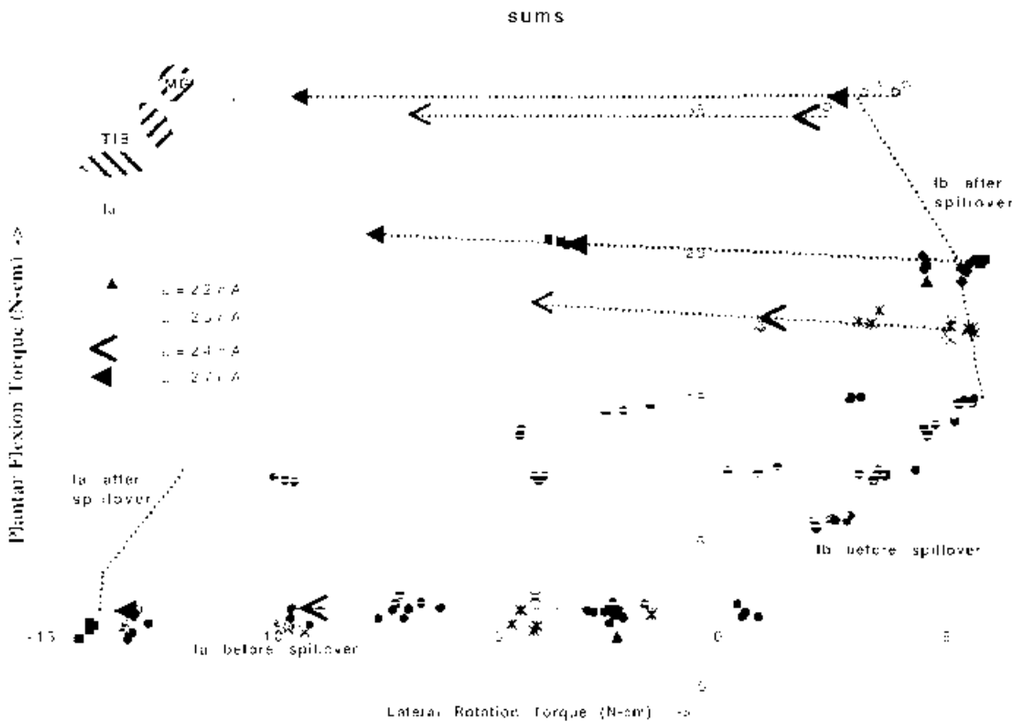

Figure C.5 – The results of stimulating two different configurations (Ia and Ib) were found to be within the 98% confidence interval for all data sets within the shaded parallelogram. Of the 6 cases where Ib was stimulated at a level that was after spillover, 4 cases produced output that was not within the 98% confidence interval. The dotted vector lines approximate the magnitude of torque output that Ia should have added. The 2 cases that were within the 98% confidence interval (noted with the vertical arrows) used small current amplitudes on Ia (2207 and 2305 μAmps). It is possible that even though Ib had reached spillover, the fibers that were activated by Ia and Ib were still partially or completely mutually exclusive. An illustration of this concept is shown in the upper left corner.

REFERENCES

Balakrishnan, N. ed., Recent Advances in Life-Testing and Reliability. Boca Raton: CRC Press, 1995.

Bishop, Michael L. ed. et al, Chemical Chemistry: principles, procedures, correlations, 2nd ed., Philadelphia: J.B. Lippincott Co., 1992, p.270.

de Putter, C. ed. et al, "Implant Materials in Biofunction", Advances in Biomaterials, vol.8, 1988, pp.377-380.

Donahue, John and Apostolou, Spiro, "Predicting Shelf Life from Accelerated Aging Data: The D&A and Variable Q_{10} Techniques", Medical Device & Diagnostic Industry, June 1998, pp. 68-72.

Edel, David. PI for NIH Contract regarding accelerated aging of *in vivo* materials.

Gamble, James Lawder, Chemical Anatomy Physiology and Pathology of Extracellular Fluid; a lecture syllabus, 5th ed., Cambridge: Harvard University Press, 1947.

Guyton, Arthur C. and Hall, John E., Textbook of Medical Physiology, 9th ed., Philadelphia: W.B. Saunders Co., 1996, pp. 301.

Hemmerich, Karl J., "General Aging Theory and Simplified Protocol for Accelerated Aging of Medical Devices," Medical Plastics and Biomaterials, July/August 1998.

Homsy, C.A. et al, "Biochemical Engineering, Materials Screening and Monitoring", Journal of Biomedical Materials Research, vol.3, 1969, pp 235-245.

Homsy, Charles A., "Biocompatibility in Selection of Materials for Implantation", Journal of Biomedical Materials Research, vol.4, 1970, pp 341-356.

Larsen, F.R. and Miller, James, "Time-Temperature Relationship for Rupture and Creep Stresses", ASME Transactions, vol. 74, 1952.

Liang, D.H., G.T.A. Kovacs, C.W. Storment, and R.L. White. A Method for Evaluating the Selectivity of Electrodes Implanted for Nerve Simulation. IEEE Trans. Biomed. Eng. 38(5):443-449, 1991.

Nelson, Wayne, Accelerated Testing:Statistical Models, Test Plans, and Data Analyses, New York: John Wiley & Sons, 1990.

Parenti, Dave, NAMSA, 770-427-3101.

Peckham, P.H. Electrical Excitation of Skeletal Muscle: Alterations in Force, Fatigue, and Metabolic Properties. Doctoral Thesis. Dept. Biomed. Eng. Case Western Reserve University.

1972.

Rutten, W.L.C., H.J. van Wier, and J.H.M. Put. Sensitivity and Selectivity of Intraneural Stimulation Using a Silicon Electrode Array. IEEE Trans. Biomed. Eng. 38(2):192-198, 1991.

Ward, Thomas Carl and Perry, John Timothy, "Dynamic Mechanical Properties of Medical Grade Silicone Elastomer Stored in Simulated Body Fluids", Journal of Biomedical Materials Research, vol.15, 1981, pp.511-525.

Yoshida, K., and K. Horch. Selective Stimulation of Peripheral Nerve Fibers using Dual Intrafascicular Electrodes. IEEE Trans. Biomed. Eng. 40(5):492-494, 1993.